TAT Conjugated MnO@PMAO for Molecular and Cellular MRI

R. Prades[1], S. L. Quinn[2], E. Giralt[1], and E. M. Shapiro[2,3]

[1]Department of Chemistry, IRB Barcelona, Barcelona, Barcelona, Spain, [2]Department of Diagnostic Radiology, Yale University School of Medicine, New Haven, CT, United States, [3]Department of Biomedical Engineering, Yale University, New Haven, CT, United States

INTRODUCTION: Environmentally responsive MRI contrast agents are attractive for molecular and cellular imaging**.** Inorganic manganese oxide particles are an example of contrast agent that can respond pH (Shapiro, et al, *MRM* 2008). These particles have very low r_1 molar relaxivity as intact particles, however, after cellular internalization and localization within endosomes and/ or lysosomes, the particles are dissolved in the predominantly acidic environment, releasing Mn^{2+} ions, which have high r_1 molar relaxivity. However the potential use *in vitro* and *in vivo* of these types of particles is limited by insolubility in aqueous solvents. Here we describe the use of Poly(maleic anhydride alt-1-ter-octadecene) (PMAO) (Moros, et al, *Nanoscale* 2010) as a coating agent for MnO nanoparticles in order to make the particles stable in aqueous buffer and subsequent conjugation of the surface nanoparticle (NPs) with targeting moieties, in this case with TAT peptide, a high efficient cell-penetrating peptide. We demonstrate how these PMAO coated manganese oxide particle have a low r_1 molar relaxivity as intact particles and elicit high r_1 molar relaxivity upon dissolution in acidic media. We then demonstrate the capability of these conjugated particles as a contrast agent for *in vivo* liver imaging. The ability of the particles decorated with TAT peptide to enhance cellular uptake *in vivo* is discussed.

MATERIALS AND METHODS: Uniform MnO nanocrystals were synthesized by controlled thermal decomposition of manganese (II) acetylacetonate in the presence of oleic acid. MnO NPs were coated with PMAO by mixing this amphipathic polymer with the NPs, afterwards the anydride of the polymer was hydrolyzed by increasing the pH, obtaining NPs stable in aqueous solvents. The NPs were also conjugated with TAT peptide by means of water soluble carbodiimides, and non-reacted points of the coating polymer were capped with glucose or PEG (750 Da) in order to give extra stability to the NPs in aqueous solvents. To measure the longitudinal MRI properties of dissolving particles, NPs were suspended in PBS pH 7.4 and 20 mM sodium citrate pH 5.5, which mimic the cytosolic and endosomal cellular compartments, respectively. Serial T_1 measurements were acquired over 60 minutes. The potential toxicity of the conjugate was assayed by MTT and neutral red toxicity assays in MCF-7 cancer cells and STO fibroblasts after a 24-hour incubation. For *in vivo* MRI, conjugated NPs were intravenously (iv) injected to CD1 mice at age 5 weeks and the liver was imaged using a T_1-weighted sequence during 3 hours on a 4 Tesla magnet. A dose of 0.250 mg Mn^{2+} (based on the content of Mn in the NP by ICP) was injected to mice.

RESULTS and DISCUSSION: TEM revealed that MnO nanocrystals were 10-20 nm (Fig 1A). XRD confirmed the crystal structure and molecular identity of MnO nanocrystals. PMAO coating was able to phase transfer MnO cores from hexane to water (Fig 1B). The hydrodynamic radius (hr) of the PMAO coated particles determined by DLS was 269.1 ± 3.1 nm and ζ-potential was -28.15 ± 0.69 mV. Intact NPs had a very low r_1 of 0.19 $mM^{-1}s^{-1}$, as expected. To assess the dissolution characteristics of the particles, a controlled release experiment was performed. Particles in the citrate buffer pH 5.5 showed significant and fast evolution of Mn^{2+} in a few minutes, whereas, particles incubated in PBS pH 7.4 did not.

NPs were decorated with TAT peptide after which the unreacted points of the coating polymer were capped by either PEG or glucose in order to increase the stability of the conjugated NPs. Conjugated NPs with TAT and glucose showed a hr of 294.3 ± 2.2 nm and a ζ-potential of 8.6 ± 0.09 mV, whereas for the conjuagate with TAT and PEG hr and ζ-potential were 314.8 ± 7.3 nm and 9.4 ± 0.21 mV, respectively, confirming the coupling of the moieties to the NPs. Both conjugates show a high stability in water and low cytotoxicity in MCF7 and STO cell lines after 24 hours incubation at 5 mM Mn.

Mice injected with particles without peptide or PEG/glucose decoration died in a few minutes after iv injection, probably due to the agglomeration of the NPs in the blood stream, whereas the animals that were injected with PEG or glucose decorated particles survived for several days. After iv injection the liver of the animals were serially imaged for 3 hours, and again at 24 hours. Images in Figure 3 demonstrate that NPs decorated with TAT and either PEG or glucose are rapidly trapped by the liver, likely due to the relative high hr of the particles. Figure 4 shows ROI analyses of liver from these animals and animals injected with MnO@PMAO particles decorated with either PEG or glucose alone. The normalized signal intensities of the liver from the animals injected with TAT decorated particles initially increases, then decreases 50% after 90 minutes (blue and red lines), while animals injected with non-TAT decorated particles remains high (black and green lines). We interpret this to be enhanced endocytosis of TAT decorated particles by liver cells, resulting in quenching of the relaxivity of the agent, similar to the phenomenon observed with intracellular Gd agents (Geninatti Crich, et al, *J Inorg Biol Chem* 2005). Signal intensity of the livers returned to baseline 24 hours after injection.

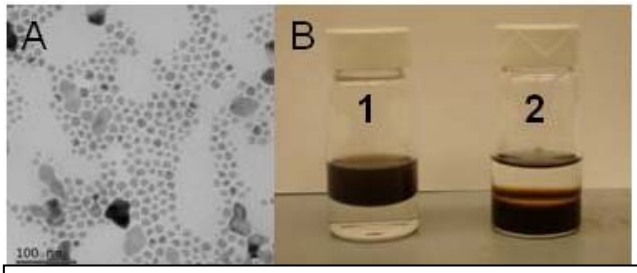

Figure 1: A) TEM of 10-20 nm MnO cores B) Phase transfer of MnO NPs by PMAO coating: 1: MnO NPs in hexane(top)/water(bottom); 2: MnO@PMAO NPs in hexane/water fully phase transferred.

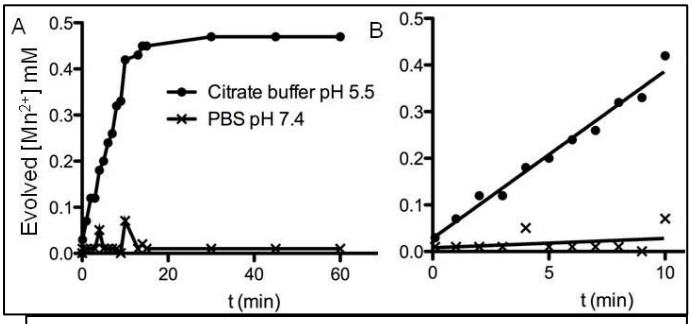

Figure 2: Dissolution studies of MnO@PMAO NPs in citrate buffer and PBS. A) 60 minute data. B) Expansion of first 10 minutes. Rapid dissolution only occurred in citrate buffer. r_1 of Mn^{2+} = 7 $mM^{-1}sec^{-1}$

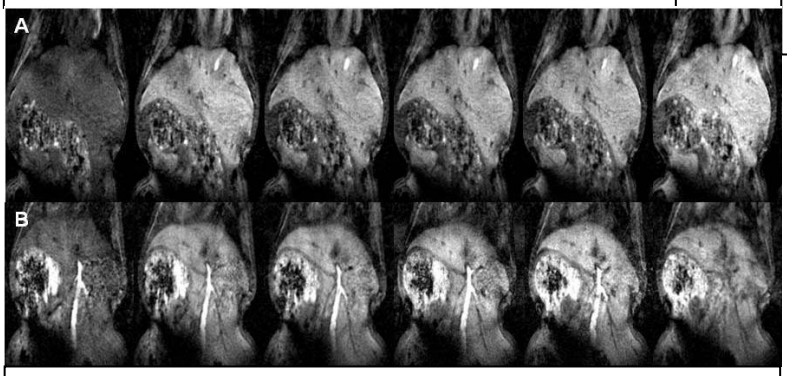

Figure 3: MRI of A) MnO@PMAO-TAT/PEG and B) MnO@PMAO-TAT/Glucose in mice. From left to right: 0, 15, 30, 60, 120 and 180 minutes after injection.

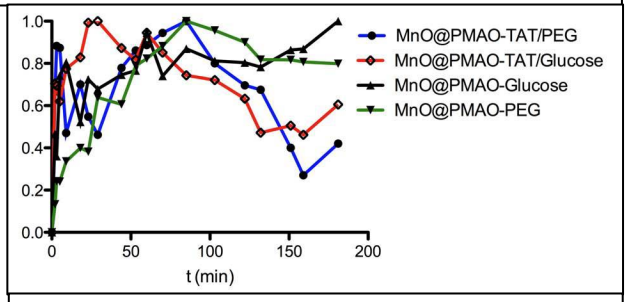

Figure 4: ROI analysis of normalized liver signal.

NIH grants P30 NS052519 and DP2 OD004362